

---

# Efficient Federated Class-Incremental Learning of Pre-Trained Models via Task-agnostic Low-rank Residual Adaptation

---

Feng Yu<sup>1\*</sup> Jia Hu<sup>1</sup> Geyong Min<sup>1</sup>  
<sup>1</sup>University of Exeter

## Abstract

Federated Parameter-Efficient Fine-Tuning (FedPEFT) reduces communication and computation costs in federated fine-tuning of pre-trained models by updating only a small subset of model parameters. However, existing approaches assume static data distributions, failing to adequately address real-world scenarios where new classes continually emerge, particularly in Federated Class Incremental Learning (FCIL). FCIL faces two key challenges: catastrophic forgetting and performance degradation caused by non-IID data across clients. Unlike current methods that maintain separate task-specific components or suffer from aggregation noise during parameter aggregation, we propose Federated Task-agnostic Low-rank Residual Adaptation (Fed-TaLoRA), a novel parameter-efficient approach for fine-tuning in resource-constrained FCIL scenarios. Specifically, we fine-tune only shared task-agnostic LoRA parameters across sequential tasks, effectively mitigating catastrophic forgetting while enabling efficient knowledge transfer among clients. Based on a theoretical analysis of aggregation, we develop a novel residual weight update mechanism that ensures accurate knowledge consolidation with minimal overhead. Our methodological innovations are attributed to three key strategies: task-agnostic adaptation, post-aggregation model calibration, and strategic placement of LoRA modules. Extensive experiments on multiple benchmark datasets demonstrate that Fed-TaLoRA consistently outperforms state-of-the-art methods in diverse data heterogeneity scenarios while substantially reducing resource requirements.

## 1 Introduction

Pre-Trained Models (PTMs) [18], including Vision Transformer (ViT) [12] and BERT [8], have revolutionized many fields such as computer vision [13] and natural language processing [37] through their powerful representations and adaptability, achieving state-of-art performance across a wide range of tasks [40, 5]. PTMs typically require fine-tuning - a process of adjusting pre-trained parameters on task-specific data to adapt general knowledge to achieve optimal performance for downstream tasks. However, traditional centralized fine-tuning of PTMs raises significant privacy concerns by requiring task data collection on central servers. Federated Learning (FL) [36] addresses these concerns by enabling collaborative model training without sharing raw data, thereby complying with data protection regulations such as GDPR [43].

While FL mitigates privacy issues, directly fine-tuning entire PTMs in federated settings introduces substantial costs, including significant communication overhead and computational demands on resource-constrained FL clients. To address these challenges, Federated Parameter-Efficient Fine-Tuning (FedPEFT) [54] leverages techniques such as prefix tuning [30], adapter tuning [20], and

---

\*Correspondence: fy274@exeter.ac.uk

low-rank adaptation (LoRA) [21] to reduce costs by freezing most PTM parameters while updating only a small subset for downstream tasks [9].

However, existing FedPEFT methods [54, 2, 5, 52, 42, 19, 48, 58, 6] typically assume static data distributions on clients, neglecting real-world scenarios where data with new classes continuously emerge [45]. Consequently, these methods struggle to adapt global models to classify all previously encountered classes as tasks evolve with new classes. Class Incremental Learning (CIL) [35, 57] offers a promising approach by enabling models to incrementally learn new classes over time. While combining FedPEFT with CIL offers a straightforward approach to incrementally adapt PTMs to tasks with new classes in federated contexts, this integration presents two significant challenges: catastrophic forgetting where fine-tuned models lose previously knowledge when acquiring new tasks; and the non-IID nature of federated data, which affects effective model training and aggregation.

These challenges are fundamental to Federated Class Incremental Learning (FCIL) [11, 46, 50], where recent popular methods address them by applying PEFT techniques to pre-trained models [16, 3, 17, 34]. Some studies [3, 17, 34] select adapters from maintained pools based on input-adapter similarity, incurring additional memory cost and inference delays. Others such as PLoRA [16] preserve learned knowledge for each task via a series of LoRA matrices, however, it increases resource costs of computation, communication, and storage through its class-specific prototype learning mechanism. Importantly, these methods store task-specific knowledge in orthogonal components through *task-specific fine-tuning followed by adaptation*, which underperforms in FCIL settings with non-IID data due to an inherent trade-off: components must adapt to local data distributions while maintaining global consistency after aggregation, resulting in sub-optimal performance. Moreover, naive weighted averaging of local LoRA parameters creates aggregation noise in non-IID settings due to a fundamental mathematical inconsistency: averaging client-specific LoRA parameters before multiplication yields different results than averaging their products [42, 48]. This discrepancy is an artifact of client drift, where local models diverge from one another and from the global representation due to data heterogeneity [55, 44].

To address the limitations of ineffective knowledge transfer among clients, inaccurate parameter aggregation in FCIL, and low resource efficiency in FCIL, we propose **Federated Task-agnostic Low-rank Residual Adaptation (Fed-TaLoRA)**, a novel parameter-efficient approach for fine-tuning PTMs in resource-constrained FCIL scenarios. Unlike existing methods that maintain separate task-specific components for each task, Fed-TaLoRA continuously fine-tunes shared task-agnostic LoRA parameters across sequential tasks, effectively mitigating catastrophic forgetting while enabling efficient knowledge transfer among clients at a minimal resource cost. We introduce a theoretically-grounded residual weight update mechanism (ResWU) that ensures accurate model consolidation with minimal computational overhead. Our work includes key innovations on *task-agnostic adaptation*, *post-aggregation model calibration*, and *strategic LoRA placement* that offer new efficiency-performance perspective for resource-constrained FCIL scenarios. Extensive experiments on four benchmark datasets demonstrate Fed-TaLoRA outperforms state-of-the-art methods by up to 21.5% in accuracy while reducing communication and computation costs by 53% and 14%, respectively.

Our main contributions are as follows:

- We propose Fed-TaLoRA, which tunes only task-agnostic LoRA parameters in FCIL with a theoretically-grounded ResWU mechanism. Fed-TaLoRA ensures accurate model consolidation to mitigate client drift in heterogeneous data settings while eliminating the need for task-specific parameters, delivering superior performance and efficiency in resource-constrained FCIL scenarios.
- We advance FCIL through three key innovations: (1) *task-agnostic adaptation* that surpasses existing methods requiring separate task-specific components in terms of accuracy, communication overhead, and storage requirements; (2) *post-aggregation model calibration* to explicitly address client drift caused by data heterogeneity; and (3) *strategic LoRA placement* across transformer blocks and feed-forward networks to optimize the performance-efficiency trade-off while preserving learned knowledge.

## 2 Related Work

**Federated Class-Incremental Learning (FCIL)** enables privacy-preserving model adaptation to new classes across distributed clients. Early approaches like GLFC [11] and LGA [10] relied on

privacy-compromising rehearsal buffers [38]. Privacy-preserving alternatives emerged through generative models (TARGET [53]) and prototypical knowledge transfer (FedProK [15]), but introduced significant computational overhead. Recent pre-trained model adaptations achieve better performance with reduced computational costs, yet face trade-offs between inference efficiency and memory requirements [34, 3, 17, 16].

**Federated Parameter-Efficient Fine-Tuning** adapts PEFT techniques to federated contexts with resource constraints [54, 5]. Research revealed that directly aggregating local LoRA parameters introduces noise in non-IID settings [2, 42]. Proposed solutions either constrain the model capacity by freezing initialized matrices [42, 19] or increase communication costs through stacking-based aggregation [48]. Our approach achieves accurate parameter aggregation without substantial overhead while effectively addressing incremental tasks challenges.

**PEFT-based FCIL** approaches [34, 3, 17] encode task-specific knowledge in modular parameters, reducing forgetting but introducing inference delays through similarity matching. PLoRA [16] addresses latency issues but requires additional prototype parameters. Existing approaches following the *task-specific fine-tuning followed by adaptation* pattern may be suboptimal for FCIL settings with non-IID data [32, 49]. Fed-TaLoRA diverges from this paradigm by continuously fine-tuning task-agnostic LoRA parameters, enabling effective knowledge transfer while balancing performance and resource efficiency.

### 3 Preliminaries

**Federated Class-Incremental Learning** is a challenging and realistic setting where a global model is collaboratively learned over a sequence of incremental tasks that introduce new classes across different clients. In this setting, suppose that there are  $K$  clients and a global server  $\mathcal{S}$ , each client  $k \in [1, K]$  trains its local model parameters  $\theta_k^t$  over its own stream dataset  $\mathcal{D}_k = \{\mathcal{D}_k^t\}_{t=1}^T$ , which consists of a sequence of  $T$  incremental tasks  $\{1, 2, \dots, t, \dots, T\}$ . For  $t$ -th task, the dataset of  $k$ -th client  $\mathcal{D}_k^t = \{\mathcal{X}_k^t, \mathcal{Y}_k^t\}$  contains  $N_k^t$  pairs of training samples  $x_i^t$  and corresponding label  $y_i^t$ , where  $\mathcal{Y}_k^t \in \mathcal{C}_k^t$  and  $\mathcal{C}$  denotes the class set. Importantly, the class sets of different tasks are disjoint and the distribution of different clients within the same task is non-IID. Suppose that  $\mathcal{L}$  is a pre-defined loss function on the current dataset  $\mathcal{D}_k^t$ , the objective of local clients is to avoid interference and absorb knowledge from previously learned tasks, which can be formulated as follows:

$$\arg \min_{\theta_k^t} \mathcal{L}(\theta_k^t; \theta_s^{t-1}, \mathcal{X}_k^t, \mathcal{Y}_k^t), \quad (1)$$

where  $\theta_s^{t-1}$  is the global model of the previous task. After the local training for the current task is complete, each client  $k$  transmits the updated model parameters  $\theta_k^t$  to the server  $\mathcal{S}$ , and server  $\mathcal{S}$  aggregates them into the global model  $\theta_s^{t+1}$  with a weighting parameter  $\omega_k$  to integrate the task knowledge across all clients as follows:

$$\theta_s^{t+1} = \sum_{k=1}^K \omega_k \theta_k^t, \text{ where } \omega_k = \frac{N_k^t}{\sum_{k=1}^K N_k^t}. \quad (2)$$

Then, the server  $\mathcal{S}$  distribute the global parameter  $\theta_s^{t+1}$  to all clients for learning the next task. After learning all tasks, the final global model aims to classify test samples of all seen classes and address the data heterogeneity while maintaining a low communication cost. Notably, in FCIL, the task identity is not known at inference.

## 4 Our Approach

### 4.1 Continually Fine-Tune Task-Agnostic LoRA of Pre-Trained Models

**Task-Agnostic LoRA.** Inspired by [21, 51], we incorporate task-agnostic LoRA (TaLoRA) of PTMs into the federated class incremental learning paradigm. Our approach is based on the hypothesis that weight updates during adaptation possess a low “intrinsic rank”. We denote the pre-trained weight matrix  $\mathbf{W} \in \mathbb{R}^{d,k}$  and the parameter update shared across all tasks and clients as  $\Delta \mathbf{W}$ . To reduce computational complexity, we constrain the parameter updates by representing  $\Delta \mathbf{W}$  through a low-rank decomposition during different task phases:

$$\mathbf{W} + \Delta \mathbf{W} = \mathbf{W} + \mathbf{B}\mathbf{A}. \quad (3)$$

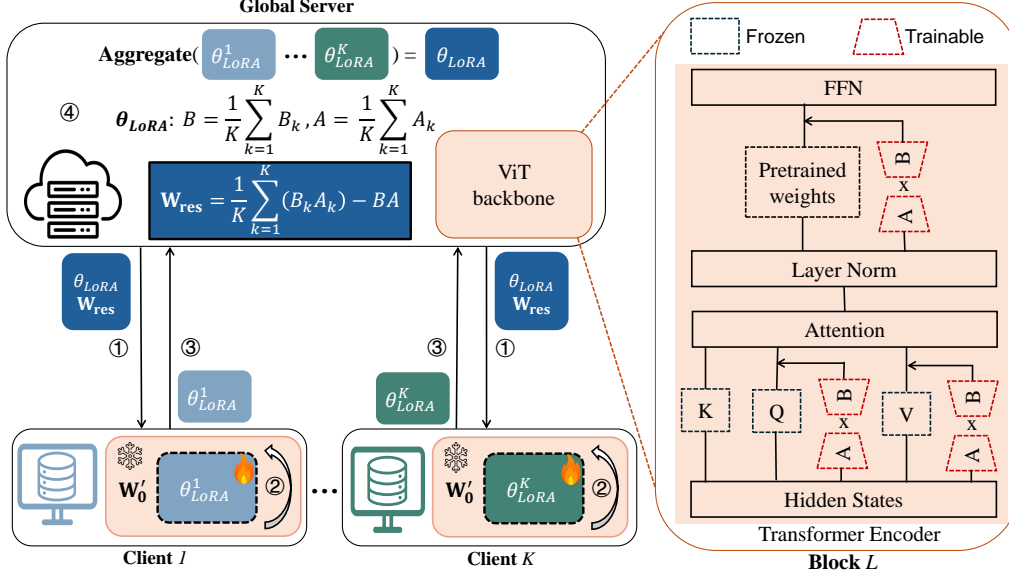


Figure 1: Pipeline of Fed-TaLoRA for FCIL. Clients first receive the global model and fine-tune only their local LoRA parameters embedded in attention layers and FFN (① → ②) on own private data containing new classes, then upload these updates (③) for server-side aggregation (④). Additionally, the server computes residual weights to capture cross-client variations, preparing an enhanced model of the next training round.

Here,  $\mathbf{B} \in \mathbb{R}^{d,r}$  and  $\mathbf{A} \in \mathbb{R}^{r,k}$ , where  $\text{rank } r \ll \min(d, k)$ . We initialize matrix  $\mathbf{B}$  with zeros and matrix  $\mathbf{A}$  with random Gaussian values, ensuring that  $\Delta \mathbf{W} = \mathbf{B} \mathbf{A}$  equals zero at the beginning of training at the server side. The pre-trained ViT backbone [12] with these embedded low-rank matrices  $\mathbf{B}$  and  $\mathbf{A}$  is then distributed to all participating clients for local training. During local training, only the two low-rank matrices  $\mathbf{B}$  and  $\mathbf{A}$  can be trained, rather than the complete set of weight parameters in attention layers and feed-forward networks (FFN). This approach restricts  $\Delta \mathbf{W}$  to rank  $r$  and reduces the total number of trainable parameters from  $d \cdot k$  to  $r \cdot (d + k)$ , thereby avoiding the computational expense of fully fine-tuning the PTM weights. Importantly, all clients collaborate on training shared task-agnostic LoRA parameters across incremental tasks, rather than maintaining separate LoRA parameters for each task in each communication round.

We argue that the weight parameters in the attention layers and the FFN modules impose significant resource usage including computational and communication costs in FL environments. Our empirical investigations in Appendix C.2 reveal that extending LoRA to the fully connected layers within FFNs substantially improves model performance, aligning with findings reported by [14, 33, 1]. Consequently, our approach enables all participating clients to continuously fine-tune task-agnostic LoRA parameters embedded in both attention layers and fully connected layers throughout the incremental learning process.

## 4.2 Residual Weight Update of Pre-Trained Models

When deploying LoRA-based methods in federated settings with non-IID data, naive parameter aggregation introduces mathematical inconsistencies that degrade model performance [2, 42]. This occurs because independently averaging low-rank matrices  $\mathbf{A}$  and  $\mathbf{B}$  across clients creates a critical discrepancy: the average of matrix products  $\frac{1}{K} \sum_{k=1}^K (\mathbf{B}_k \mathbf{A}_k)$  differs from the product of averaged matrices  $\frac{1}{K} \sum_{k=1}^K \mathbf{B}_k \times \frac{1}{K} \sum_{k=1}^K \mathbf{A}_k$ . Previous approaches either compromise LoRA’s efficiency benefits, limit model expressivity by fixing certain parameters [42, 58, 19], or increase communication overhead through a complex aggregation scheme [48]. More detailed theory analysis of LoRA-based aggregation can be found in Appendix A.

To achieve accurate aggregation with tiny overhead, we introduce the Residual Weight Update (ResWU) mechanism. Beyond aggregating the low-rank matrices ( $\mathbf{B} = \frac{1}{K} \sum_{k=1}^K \mathbf{B}_k$  and  $\mathbf{A} =$

---

**Algorithm 1** Training Algorithm of Fed-TaLoRA

---

**Inputs:** Training dataset  $\mathcal{D}_k^t$  of client  $k$  for task  $t = 1, \dots, T$ ; Communication round  $R$ ; Local epoch number  $\varepsilon$ ; Global network  $M_\theta(\cdot) = h_{\theta_{cls}}(f_{\theta_{rps}}(\cdot))$  with PTM parameters containing frozen and LoRA parameters  $\theta_{rps} = \{\theta_f, \theta_{LoRA}\}$ ; learning rate  $\eta_1$  for  $\theta_{rps}$  and  $\eta_2$  for  $\theta_{cls}$  ( $\eta_1 < \eta_2$ ).

**ClientLocalTuning** ( $t, k, \theta_{LoRA}^r, \mathbf{W}_{res}$ )

- 1: Update the pre-trained weights  $\mathbf{W}_0$  by Eq. (5) ▷ Residual weight update
- 2:  $\theta_k^r \leftarrow$  (assemble  $\theta_{LoRA}^r$  and  $\theta_f$ )
- 3: **for** epoch  $e = 1$  to  $\varepsilon$  **do**
- 4:    $\theta_{LoRA}^{r+1} \leftarrow$  tuning  $\theta_{k,r+1} = (\theta_{LoRA}^r, \theta_{cls})$  on  $\mathcal{D}_k^t$  ▷ learning rate  $\eta_1$  for  $\theta_{LoRA}^{r+1}$  and  $\eta_2$  for  $\theta_{cls}$
- 5: **end for**
- 6: **Send**  $\theta_{LoRA}^{r+1}$  to the server

**ServerGlobalAggregation**

- 7: **for** task  $t = 1, \dots, T$  **do**
- 8:   **for** round  $r = 1$  to  $R$  **do**
- 9:      $U^r \leftarrow$  (randomly sample  $K$  clients from  $U$ )
- 10:    **for** client  $k \in U^r$  **do** ▷ Non-IID data across clients
- 11:     **ClientLocalTuning** ( $t, k, \theta_{LoRA}^r, \mathbf{W}_{res}$ ) ▷ Fine-tune task-agnostic LoRA
- 12:    **end for**
- 13:    Receive local updated parameters  $\theta_{LoRA}^{k,r}$
- 14:    Perform global aggregation by Eq. (9)
- 15:    Compute the residual weight by Eq. (4)
- 16:   **end for**
- 17: **end for**

**Output:**  $M_\theta^*$

---

$\frac{1}{K} \sum_{k=1}^K \mathbf{A}_k$ ), the server computes a residual weight:

$$\mathbf{W}_{res} = \frac{1}{K} \sum_{k=1}^K (\mathbf{B}_k \mathbf{A}_k) - \frac{1}{K} \sum_{k=1}^K \mathbf{B}_k \times \frac{1}{K} \sum_{k=1}^K \mathbf{A}_k = \frac{1}{K} \sum_{k=1}^K (\mathbf{B}_k \mathbf{A}_k) - \mathbf{B} \mathbf{A}. \quad (4)$$

This residual weight is distributed to clients along with the aggregated LoRA parameters. Clients then update their pre-trained weights:

$$\mathbf{W}'_0 = \mathbf{W}_0 + \mathbf{W}_{res}, \quad (5)$$

before training LoRA parameters on their private datasets, where  $\mathbf{W}_0$  denotes the frozen pre-trained weights in the pre-trained model. This mechanism can ensure accurate aggregation for each client:

$$\mathbf{W}_g = \mathbf{W}'_0 + \mathbf{B} \mathbf{A} = \mathbf{W}_0 + \mathbf{W}_{res} + \mathbf{B} \mathbf{A} = \mathbf{W}_0 + \frac{1}{K} \sum_{k=1}^K (\mathbf{B}_k \mathbf{A}_k) \stackrel{\text{Eq. (8)}}{=} \mathbf{W}_g^*. \quad (6)$$

In this way, we theoretically achieve accurate aggregation for each communication round in heterogeneous data distribution scenarios.

Our **Fed-TaLoRA** learning procedure follows a systematic communication protocol between the server and clients. The process begins with the server initializing a pre-trained model trainable task-agnostic LoRA parameters  $\theta_{LoRA}$  and frozen backbone parameters  $\theta_f$ , which is then distributed to all participating clients. Upon receipt, clients first apply the computed residual weight  $\mathbf{W}_{res}$  to update their pre-trained weights  $\mathbf{W}_0$ , ensuring mathematical consistency across the federation. Clients then fine-tune the task-agnostic LoRA parameters on their private datasets across different incremental task phases. Following local optimization, only the updated LoRA parameters are transmitted back to the central server, where weighted averaging performed to aggregate to collect knowledge. The server subsequently computes a new residual weight for the next communication round. This iterative process continues until model convergence is achieved. Notably, in IID data distribution scenarios,  $\mathbf{W}_{res}$  can be simplified to zero. Figure 1 provides a visual illustration of the complete Fed-TaLoRA pipeline, with the formal algorithmic implementation detailed in Algorithm 1.

Table 1: Results (%) on CIFAR-100 including 10 tasks (10 classes per task) and under different degree of two non-IID setting.  $\alpha$  denotes the number of different labels for each client,  $\beta$  denotes a concentration parameter controlling Dirichlet distribution.

Non-IID Partition Method	Quantity-based label imbalance						Distribution-based label imbalance					
	$\alpha = 6$		$\alpha = 4$		$\alpha = 2$		$\beta = 0.5$		$\beta = 0.1$		$\beta = 0.05$	
	FAA	AIA	FAA	AIA	FAA	AIA	FAA	AIA	FAA	AIA	FAA	AIA
Joint	88.6	-	84.3	-	79.8	-	90.1	-	87.8	-	85.9	-
EWC+FL	57.9	69.1	55.9	66.8	42.2	52.7	65.5	77.8	57.8	73.2	43.5	59.2
LwF+FL	57.4	68.8	55.1	66.7	40.8	52.9	64.7	77.5	54.6	63.3	45.7	64.5
iCaRL+FL	35.8	56.5	37.1	58.9	43.4	55.3	51.3	67.7	50.1	65.9	44.6	63.0
L2P+FL	63.4	65.1	59.0	58.2	2.6	5.6	53.9	51.6	62.9	71.4	38.7	32.2
FedCLM	58.9	69.4	57.6	67.6	44.3	57.9	66.5	77.4	61.0	71.8	48.8	63.5
FedNCM	65.6	74.4	61.9	71.1	49.6	59.8	66.8	77.9	62.1	72.4	50.9	65.9
TARGET	60.9	71.3	58.8	69.5	45.2	56.5	66.1	77.8	60.5	71.1	51.8	65.3
GLFC	58.2	70.4	53.7	65.9	13.1	37.7	-	-	-	-	-	-
LGA	64.5	73.6	61.1	70.5	21.6	40.9	-	-	-	-	-	-
PILoRA	69.5	78.6	65.1	74.4	54.9	62.6	68.5	78.1	63.4	73.7	54.8	67.1
<b>Fed-TaLoRA</b>	<b>76.6</b>	<b>84.2</b>	<b>72.9</b>	<b>81.0</b>	<b>66.5</b>	<b>73.2</b>	<b>77.4</b>	<b>85.5</b>	<b>76.8</b>	<b>84.1</b>	<b>75.3</b>	<b>83.3</b>

## 5 Experiments

### 5.1 Experimental Settings

**Benchmark.** Following [16], we use CIFAR-100 [24], Tiny-ImageNet [25], ImageNet-Subset [22], and ImageNet [7] datasets in our experiments. For a fair comparison with the baseline class-incremental learning methods in the FCIL setting, we follow the same protocols proposed by [56] to split 10 incremental tasks, and utilize the same class order generated from [56]. Additionally, we distribute the data of each task across 10 clients, employing the widely adopted non-IID settings: *distribution-based label imbalance* and *quantity-based label imbalance* [29]. The former partitions the data based on a Dirichlet distribution controlled by the parameter  $\beta$ , while the latter ensures that each client contains exactly  $\alpha$  classes within each task. We assess all methods across 6 different scenarios of non-IID for each dataset. Specifically, for distribution-based label imbalance settings, we set  $\alpha \in \{2, 4, 6\}$  for CIFAR-100, and  $\alpha \in \{4, 8, 12\}$  for Tiny-ImageNet. On both datasets, we conduct experiments with  $\beta \in \{0.05, 0.1, 0.5\}$ . Please find extended experimental results on ImageNet-Subset and ImageNet datasets in Appendix D.

**Baseline.** We compare the proposed method with existing FCIL methods: TARGET [53], GLFC [11], LGA [10], and PILoRA [16]. We adopt several representative CIL methods: EWC [23], LwF [31], iCaRL [41], L2P [47], which were originally designed for class-incremental learning, and FL method FedNCM [28] and its variant FedCLM [28] in the FCIL setting. We tune all methods with the same pre-trained model as ours and fine-tune them using LoRA for a fair comparison.

**Metrics.** We report two widely adopted metrics in the FCIL setting: Final Average Accuracy (FAA) and Average Incremental Accuracy (AIA). FAA is the accuracy of all seen classes in the final task and AIA is calculated as the average accuracy of all tasks (equivalent to ‘ $A_N$ , Avg.’ in [16, 51]).

**Implementation.** All experiments are implemented using PyTorch [39]. Following previous works [51, 16] and considering the potential data leakage issue, we evaluate the performance of our method with self-supervised pre-trained weights of DINO [4] for ViT-B/16 [12]. An SGD optimizer is used for ours with the same batch size of 64 as baselines. Followed by [51], to effectively balance the preservation of pre-trained knowledge stability with the adaptability required for new tasks, we use the learning rate of 0.001 for the representation layer and 0.01 for the classification layer. We initialize 10 local clients, and the number of local training epochs is set to 5. For each task, 30 rounds of communication are set for all benchmark datasets. We conduct experiments for 3 times with 3 random seeds (1993, 1996, 1997) and report the averaged results. Results of baselines are sourced from the recent research [16]. Please refer the implementation details in Appendix B. Considering the trade-off between model performance and the number of trainable parameters, inspired by previous efforts in fixed layer select strategy for fine-tuning [26, 27], for CIFAR-100, we train LoRA in the first 4 blocks, middle 4 blocks and last 4 blocks, named **first**, **mid** and **last**; for Tiny-ImageNet, we

Table 2: Results (%) on TinyImageNet including 10 tasks (20 classes per task) and under different degrees of two non-IID settings.

Non-IID Partition Method	Quantity-based label imbalance						Distribution-based label imbalance					
	$\alpha = 12$		$\alpha = 8$		$\alpha = 4$		$\beta = 0.5$		$\beta = 0.1$		$\beta = 0.05$	
	<i>FAA</i>	<i>AIA</i>	<i>FAA</i>	<i>AIA</i>	<i>FAA</i>	<i>AIA</i>	<i>FAA</i>	<i>AIA</i>	<i>FAA</i>	<i>AIA</i>	<i>FAA</i>	<i>AIA</i>
Joint	83.6	-	82.9	-	80.2	-	84.3	-	83.3	-	82.8	-
L2P+FL	61.6	58.0	49.4	39.3	8.2	10.2	64.2	66.9	56.3	52.5	51.9	43.2
FedCLM	61.6	72.4	51.8	60.3	45.8	56.9	66.5	77.4	60.4	71.0	46.7	57.8
FedNCM	71.6	81.6	69.5	79.4	57.2	64.7	73.7	81.6	70.8	80.4	68.4	78.0
TARGET	72.6	81.6	70.3	79.6	63.8	73.5	71.6	80.9	71.0	80.1	69.3	79.1
GLFC	69.1	77.9	61.3	73.5	25.1	39.4	-	-	-	-	-	-
LGA	71.3	79.4	65.8	75.3	36.7	48.8	-	-	-	-	-	-
PiLoRA	74.4	81.0	74.3	80.9	70.1	77.8	74.5	80.9	74.3	81.0	73.6	80.2
<b>Fed-TaLoRA</b>	<b>77.2</b>	<b>83.0</b>	<b>76.2</b>	<b>82.8</b>	<b>74.1</b>	<b>80.9</b>	<b>78.0</b>	<b>83.9</b>	<b>77.0</b>	<b>82.6</b>	<b>75.5</b>	<b>81.9</b>

train LoRA in the first 6 blocks and the last 6 blocks, named **bottom** and **top**. And **first** and **bottom** are also noted as **Fed-TaLoRA** in all experiments since the LoRA module embedded in the first block is utilized in [16] for a fair comparison. Please refer to extensive experiments of the impact of LoRA embedded in the different blocks and layers in Appendix C.

## 5.2 Experimental Results

### 5.2.1 Comparable Experiments

We evaluate all methods using the *FAA* and *AIA* metrics, with comprehensive results presented in Tables 1 and 2. Our findings demonstrate that Fed-TaLoRA consistently outperforms all baseline methods across various non-IID scenarios. Among existing FCIL approaches, TARGET maintains relatively stable performance under different degrees of data heterogeneity, exhibiting notable robustness. In contrast, GLFC and LGA experience significant performance degradation when confronted with extreme quantity-based label imbalance. Although PiLoRA achieves better results than these methods, it still suffers considerable performance decline under severe heterogeneity conditions, highlighting a common limitation among current FCIL methods in handling non-IID data distributions, particularly in scenarios with extreme heterogeneity. Our method delivers substantial performance improvements over the current SOTA PiLoRA across both datasets. On CIFAR-100, Fed-TaLoRA surpasses PiLoRA by margins ranging from 7.1%  $\sim$  21.5% in terms of *FAA*. More impressively, our method maintains the superior performance even under extreme data heterogeneity where competing approaches falter significantly. On the more complex Tiny-ImageNet dataset, our method consistently outperforms PiLoRA by 1.9%  $\sim$  4.0% across all evaluated scenarios. Please find extended experimental results on ImageNet-Subset and ImageNet datasets in Appendix D. These results illustrate the efficiency of *task-agnostic adaptation*: directly fine-tuning task-agnostic parameters yield superior efficiency compared to adapting models that have undergone task-specific fine-tuning.

### 5.2.2 Ablation Study

To evaluate the effect of each component of Fed-TaLoRA, we performed an ablation study on the CIFAR-100 setup of 10 tasks. Fed-TaLoRA contains two core components, i.e., TaLoRA and ResWU. We conducted five different experiments as follows:

1. Fed-TaLoRA w/o TaLoRA and ResWU: fine-tuning the linear classifiers without applying TaLoRA and ResWU while freezing the entire backbone.
2. Fed-TaLoRA w/o TaLoRA (frozen): applying ResWU while freezing the entire backbone.
3. Fed-TaLoRA w/o ResWU: applying TaLoRA without ResWU.
4. Fed-TaLoRA (fully): applying ResWU and continually fine-tuning the entire backbone.
5. Fed-TaLoRA: applying TaLoRA and ResWU.

As shown in Table 3, the classification precision *FAA* and *AIA* of Fed-TaLoRA w/o TaLoRA and ResWU frozen decrease by 8.4% and 8.0%, respectively, compared to the method Fed-TaLoRA (fully

fine-tuning) when  $\alpha = 6$ . This suggests that the representation ability of the former method is limited, as only the classifier with few parameters is trained while most of the backbone parameters remain unchanged. In contrast, compared to fully fine-tuning, our method achieves comparable performance by tuning task-agnostic LoRA parameters at significantly lower computational and communication costs. Furthermore, our ablation studies demonstrate that without the ResWU mechanism, our method’s performance significantly degrades, particularly in terms of *AIA*. This underscores the critical role that ResWU plays in enabling accurate model aggregation at the server, thereby enhancing the model’s generalization capabilities and robustness when learning across heterogeneous data distributions.

### 5.2.3 Resource Usage Analysis

In our method, we freeze the pre-trained backbone for all clients and exclusively fine-tune task-shared LoRA parameters throughout the learning process. Additionally, we compute the residual weight updates once per communication round to mitigate aggregation inconsistencies in heterogeneous data distributions.

Table 3: Ablation Results (%) on CIFAR-100.

Partition Method	$\alpha = 6$		$\beta = 0.5$	
	<i>FAA</i>	<i>AIA</i>	<i>FAA</i>	<i>AIA</i>
w/o TaLoRA and ResWU	69.6	78.7	71.4	81.5
w/o TaLoRA (frozen)	69.8	78.9	71.4	81.5
w/o ResWU	76.5	82.9	77.4	82.8
Fed-TaLoRA (fully)	78.2	86.9	79.4	87.1
<b>Fed-TaLoRA</b>	76.6	84.2	77.4	85.5

**(1) Computation and memory efficiency.** Fed-TaLoRA achieves exceptional resource efficiency across both computation and memory dimensions. By fine-tuning only shared task-agnostic LoRA parameters and computing residual weight updates just once per communication round, our method introduces minimal overhead while maintaining superior performance. As shown in Table 4, Fed-TaLoRA requires fewer trainable parameters than competing methods. Unlike PiLoRA, which stores separate task-specific parameters and class prototypes for each incremental task, or methods like TARGET, LGA, and GFLC that require growing memory buffers for exemplar storage, Fed-TaLoRA maintains a constant memory footprint regardless of task count. This balanced efficiency in both computation and memory makes Fed-TaLoRA particularly well-suited for resource-constrained federated environments where clients have limited capabilities.

Table 4: Comparison of the number of learnable parameters of both datasets.

Method	# Params	
	CIFAR-100	Tiny-ImageNet
PiLoRA	0.21M	0.29M
<b>Fed-TaLoRA</b>	0.18M	0.27M

**(2) Communication cost.** Our empirical evaluation confirms Fed-TaLoRA’s optimal balance between communication efficiency and model performance. As detailed in Table 5, Fed-TaLoRA achieves the lowest communication overhead while simultaneously delivering superior accuracy compared to all baselines. Our ablation studies in Appendix D further demonstrate the trade-off of performance and resource costs for *strategic LoRA placement*: strategically embedding task-agnostic LoRA in a reduced subset of Transformer blocks still outperforms current SOTA while reducing additional communication and computational costs. These findings underscore the versatility and efficiency of task-agnostic adaptation within Transformer architectures and suggest promising applications beyond FCIL.

Table 5: Comparison of communication cost per round on CIFAR-100,  $\alpha = 6$ . The column of # Params is sourced from [16].

Method	#Params	<i>FAA</i>	<i>AIA</i>
GLFC	10.82M	58.2	70.4
LGA	10.82M	64.5	73.6
TARGET	4.64M	60.9	71.3
PiLoRA	0.77M	69.5	78.6
<b>Fed-TaLoRA</b>	0.36M	76.6	84.2

### 5.2.4 Further Analysis

In this section, we analyze resource usage and investigate the impact of accurate aggregation strategies and the number of local clients. Please refer to more details regarding the impact of various numbers of tasks in Appendix D.1.

**Impact of strategies for accurate aggregation.** To evaluate approaches for addressing inaccurate aggregation in LoRA-based federated fine-tuning within FCIL context, we compare our mechanism



with alternative strategies. We implemented the recent parameter-freezing approach from FFA-LoRA [42] by freezing matrix  $\mathbf{A}$  during training (denoted as ‘w/ FFA’ in Figure 2).

Figure 2 illustrates the relative final average accuracy of both alternative approaches—Fed-TaLoRA without ResWU (‘w/o ResWU’) and Fed-TaLoRA with frozen matrix  $\mathbf{A}$  (‘w/ FFA’)—against our complete Fed-TaLoRA implementation. Across all heterogeneous data scenarios, our model consistently outperforms the model with frozen matrix  $\mathbf{A}$ . This demonstrates that while simply freezing the LoRA matrix offers resource consumption advantages, it significantly degrades model performance in realistic FCIL settings — contradicting our goal of achieving an optimal balance between performance and resource efficiency in resource-constrained environments. In contrast, our ResWU mechanism functioning as the *post-aggregation model calibration* consistently enhances performance in all evaluation settings, underscoring the importance of model calibration techniques that explicitly address client drift arising from inconsistent local model optimization on heterogeneous datasets [55].

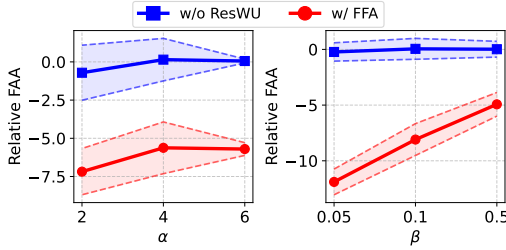


Figure 2: Relative final average accuracy (%) compared to Fed-TaLoRA on CIFAR-100.

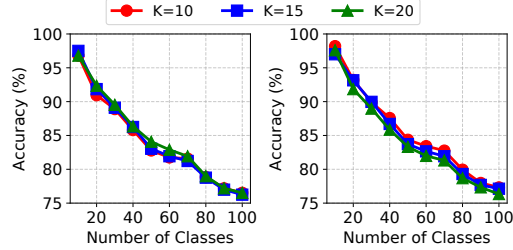


Figure 3: The impact of different number of  $K$  on CIFAR-100,  $\alpha = 6$  (left) and  $\beta = 0.5$  (right).

**Impact of the number of local clients ( $K$ ).** As illustrated in Figure 3, we investigate how varying the number of local clients ( $K = \{10, 15, 20\}$ ) affects our model’s performance on the CIFAR-100 dataset under different heterogeneity conditions. For quantity-based label imbalance ( $\alpha = 6$ ), we observe a phase-dependent pattern: during the first 5 incremental tasks, configurations with more clients achieve higher accuracy, where in the final 5 tasks, this trend reverses, with fewer clients yielding superior performance. This pattern suggests that in early learning stages, the model benefits from the richer feature representations developed from the larger aggregate sample pool available across more clients. However, as training progress through additional tasks, the representation enhancement from having more clients reaches diminishing returns, allowing the configuration with fewer clients ( $K = 10$ ) to ultimately outperform those with more clients ( $K = 15$  and  $K = 20$ ). For distribution-based label imbalance ( $\beta = 0.5$ ), we observe a slight but consistent decrease in model performance as the number of clients increases, reflecting the greater data heterogeneity introduced by distributing classes across more clients. Notably, across both heterogeneity scenarios, the variance in performance remains relatively small regardless of client count. This can be attributed to two key components: the task-agnostic nature of the trained LoRA parameters and the accurate aggregation enabled by our residual weight update mechanism, which effectively mitigates the challenges of client-count scaling.

## 6 Conclusions

We propose Fed-TaLoRA, a novel approach for FCIL that addresses the challenges of adapting pre-trained models across distributed clients. Unlike existing methods that maintain separate task-specific components, Fed-TaLoRA continuously fine-tunes shared task-agnostic LoRA parameters embedded within transformer layers, significantly mitigating catastrophic forgetting while enabling efficient knowledge transfer among clients. Our theoretical analysis reveals aggregation bias in naive parameter aggregation under non-IID settings, which we address through a residual weight update mechanism that ensures accurate knowledge consolidation with minimal overhead. We attribute our methodological innovations to *task-agnostic adaptation*, *post-aggregation model calibration* and *strategic LoRA placement*. Extensive experiments on multiple benchmark datasets demonstrate that Fed-TaLoRA consistently outperforms baselines across various data heterogeneity scenarios while substantially reducing resource costs, establishing a new efficiency-performance frontier for resource-constrained FCIL scenarios.

## References

- [1] Ahmed Agiza, Marina Neseem, and Sherief Reda. Mtlora: Low-rank adaptation approach for efficient multi-task learning. In *Proceedings of the IEEE/CVF conference on computer vision and pattern recognition*, pages 16196–16205, 2024.
- [2] Sara Babakniya, Ahmed Roushdy Elkordy, Yahya H. Ezzeldin, Qingfeng Liu, Kee-Bong Song, Mostafa EL-Khamy, and Salman Avestimehr. SLoRA: Federated Parameter Efficient Fine-Tuning of Language Models. In *International Workshop on Federated Learning in the Age of Foundation Models in Conjunction with NeurIPS 2023*, October 2023.
- [3] Gaurav Bagwe, Xiaoyong Yuan, Miao Pan, and Lan Zhang. Fed-cprompt: Contrastive prompt for rehearsal-free federated continual learning. *arXiv preprint arXiv:2307.04869*, 2023.
- [4] Mathilde Caron, Hugo Touvron, Ishan Misra, Hervé Jegou, Julien Mairal, Piotr Bojanowski, and Armand Joulin. Emerging Properties in Self-Supervised Vision Transformers. In *2021 IEEE/CVF International Conference on Computer Vision (ICCV)*, pages 9630–9640, October 2021.
- [5] Jinyu Chen, Wenchao Xu, Song Guo, Junxiao Wang, Jie Zhang, and Haozhao Wang. Fedtune: A deep dive into efficient federated fine-tuning with pre-trained transformers. *arXiv preprint arXiv:2211.08025*, 2022.
- [6] Shuangyi Chen, Yue Ju, Hardik Dalal, Zhongwen Zhu, and Ashish Khisti. Robust federated finetuning of foundation models via alternating minimization of lora. *arXiv preprint arXiv:2409.02346*, 2024.
- [7] Jia Deng, Wei Dong, Richard Socher, Li-Jia Li, Kai Li, and Li Fei-Fei. Imagenet: A large-scale hierarchical image database. In *2009 IEEE conference on computer vision and pattern recognition*, pages 248–255. Ieee, 2009.
- [8] Jacob Devlin. Bert: Pre-training of deep bidirectional transformers for language understanding. *arXiv preprint arXiv:1810.04805*, 2018.
- [9] Ning Ding, Yujia Qin, Guang Yang, Fuchao Wei, Zonghan Yang, Yusheng Su, Shengding Hu, Yulin Chen, Chi-Min Chan, Weize Chen, et al. Delta tuning: A comprehensive study of parameter efficient methods for pre-trained language models. *arXiv preprint arXiv:2203.06904*, 2022.
- [10] Jiahua Dong, Hongliu Li, Yang Cong, Gan Sun, Yulun Zhang, and Luc Van Gool. No One Left Behind: Real-World Federated Class-Incremental Learning. *IEEE Transactions on Pattern Analysis and Machine Intelligence*, 46(04):2054–2070, April 2024.
- [11] Jiahua Dong, Lixu Wang, Zhen Fang, Gan Sun, Shichao Xu, Xiao Wang, and Qi Zhu. Federated Class-Incremental Learning. In *2022 IEEE/CVF Conference on Computer Vision and Pattern Recognition (CVPR)*, pages 10154–10163, New Orleans, LA, USA, June 2022. IEEE.
- [12] Alexey Dosovitskiy, Lucas Beyer, Alexander Kolesnikov, Dirk Weissenborn, Xiaohua Zhai, Thomas Unterthiner, Mostafa Dehghani, Matthias Minderer, Georg Heigold, Sylvain Gelly, Jakob Uszkoreit, and Neil Houlsby. An Image is Worth 16x16 Words: Transformers for Image Recognition at Scale. In *International Conference on Learning Representations*, October 2020.
- [13] Yifan Du, Zikang Liu, Junyi Li, and Wayne Xin Zhao. A survey of vision-language pre-trained models. *arXiv preprint arXiv:2202.10936*, 2022.
- [14] Vlad Fomenko, Han Yu, Jongho Lee, Stanley Hsieh, and Weizhu Chen. A note on lora. *arXiv preprint arXiv:2404.05086*, 2024.
- [15] Xin Gao, Xin Yang, Hao Yu, Yan Kang, and Tianrui Li. Fedprok: Trustworthy federated class-incremental learning via prototypical feature knowledge transfer. In *Proceedings of the IEEE/CVF Conference on Computer Vision and Pattern Recognition*, pages 4205–4214, 2024.
- [16] Haiyang Guo, Fei Zhu, Wenzhuo Liu, Xu-Yao Zhang, and Cheng-Lin Liu. Pilora: Prototype guided incremental lora for federated class-incremental learning. In *European Conference on Computer Vision*, pages 141–159. Springer, 2024.

- [17] Shaunak Halbe, James Seale Smith, Junjiao Tian, and Zsolt Kira. Continual adaptation of vision transformers for federated learning. *arXiv preprint arXiv:2306.09970*, 2023.
- [18] Xu Han, Zhengyan Zhang, Ning Ding, Yuxian Gu, Xiao Liu, Yuqi Huo, Jiezhong Qiu, Yuan Yao, Ao Zhang, Liang Zhang, et al. Pre-trained models: Past, present and future. *AI Open*, 2:225–250, 2021.
- [19] Yongchang Hao, Yanshuai Cao, and Lili Mou. Flora: Low-rank adapters are secretly gradient compressors. *arXiv preprint arXiv:2402.03293*, 2024.
- [20] Neil Houlsby, Andrei Giurgiu, Stanislaw Jastrzebski, Bruna Morrone, Quentin de Laroussilhe, Andrea Gesmundo, Mona Attariyan, and Sylvain Gelly. Parameter-Efficient Transfer Learning for NLP, June 2019.
- [21] Edward J Hu, Yelong Shen, Phillip Wallis, Zeyuan Allen-Zhu, Yanzhi Li, Shean Wang, Lu Wang, and Weizhu Chen. Lora: Low-rank adaptation of large language models. *arXiv preprint arXiv:2106.09685*, 2021.
- [22] Xinting Hu, Kaihua Tang, Chunyan Miao, Xian-Sheng Hua, and Hanwang Zhang. Distilling causal effect of data in class-incremental learning. In *Proceedings of the IEEE/CVF conference on Computer Vision and Pattern Recognition*, pages 3957–3966, 2021.
- [23] James Kirkpatrick, Razvan Pascanu, Neil Rabinowitz, Joel Veness, Guillaume Desjardins, Andrei A. Rusu, Kieran Milan, John Quan, Tiago Ramalho, Agnieszka Grabska-Barwinska, Demis Hassabis, Claudia Clopath, Dharshan Kumaran, and Raia Hadsell. Overcoming catastrophic forgetting in neural networks. *Proceedings of the National Academy of Sciences*, 114(13):3521–3526, March 2017.
- [24] Alex Krizhevsky and Geoffrey Hinton. Learning multiple layers of features from tiny images. 2009.
- [25] Ya Le and Xuan Yang. Tiny imagenet visual recognition challenge. *CS 231N*, 7(7):3, 2015.
- [26] Jaejun Lee, Raphael Tang, and Jimmy Lin. What would elsa do? freezing layers during transformer fine-tuning. *arXiv preprint arXiv:1911.03090*, 2019.
- [27] Yoonho Lee, Annie S Chen, Fahim Tajwar, Ananya Kumar, Huaxiu Yao, Percy Liang, and Chelsea Finn. Surgical fine-tuning improves adaptation to distribution shifts. *arXiv preprint arXiv:2210.11466*, 2022.
- [28] Gwen Legate, Nicolas Bernier, Lucas Page-Caccia, Edouard Oyallon, and Eugene Belilovsky. Guiding the last layer in federated learning with pre-trained models. *Advances in Neural Information Processing Systems*, 36, 2024.
- [29] Qinbin Li, Yiqun Diao, Quan Chen, and Bingsheng He. Federated Learning on Non-IID Data Silos: An Experimental Study. In *2022 IEEE 38th International Conference on Data Engineering (ICDE)*, pages 965–978, May 2022.
- [30] Xiang Lisa Li and Percy Liang. Prefix-tuning: Optimizing continuous prompts for generation. *arXiv preprint arXiv:2101.00190*, 2021.
- [31] Zhizhong Li and Derek Hoiem. Learning without Forgetting. *IEEE Transactions on Pattern Analysis and Machine Intelligence*, 40(12):2935–2947, December 2018.
- [32] Baohao Liao, Yan Meng, and Christof Monz. Parameter-Efficient Fine-Tuning without Introducing New Latency. In Anna Rogers, Jordan Boyd-Graber, and Naoaki Okazaki, editors, *Proceedings of the 61st Annual Meeting of the Association for Computational Linguistics (Volume 1: Long Papers)*, pages 4242–4260, Toronto, Canada, July 2023. Association for Computational Linguistics.
- [33] Liting Lin, Heng Fan, Zhipeng Zhang, Yaowei Wang, Yong Xu, and Haibin Ling. Tracking meets lora: Faster training, larger model, stronger performance. In *European Conference on Computer Vision*, pages 300–318. Springer, 2024.

- [34] Chenghao Liu, Xiaoyang Qu, Jianzong Wang, and Jing Xiao. FedET: A Communication-Efficient Federated Class-Incremental Learning Framework Based on Enhanced Transformer. In *Proceedings of the Thirty-Second International Joint Conference on Artificial Intelligence*, pages 3984–3992, Macau, SAR China, August 2023. International Joint Conferences on Artificial Intelligence Organization.
- [35] Marc Masana, Xialei Liu, Bartłomiej Twardowski, Mikel Menta, Andrew D Bagdanov, and Joost Van De Weijer. Class-incremental learning: survey and performance evaluation on image classification. *IEEE Transactions on Pattern Analysis and Machine Intelligence*, 45(5):5513–5533, 2022.
- [36] Brendan McMahan, Eider Moore, Daniel Ramage, Seth Hampson, and Blaise Aguera y Arcas. Communication-efficient learning of deep networks from decentralized data. In *Artificial intelligence and statistics*, pages 1273–1282. PMLR, 2017.
- [37] Bonan Min, Hayley Ross, Elior Sulem, Amir Poursan Ben Veyseh, Thien Huu Nguyen, Oscar Sainz, Eneko Agirre, Ilana Heintz, and Dan Roth. Recent advances in natural language processing via large pre-trained language models: A survey. *ACM Computing Surveys*, 56(2):1–40, 2023.
- [38] Milad Khademi Nori, Il-Min Kim, and Guanghui Wang. Federated class-incremental learning: A hybrid approach using latent exemplars and data-free techniques to address local and global forgetting. *arXiv preprint arXiv:2501.15356*, 2025.
- [39] Adam Paszke, Sam Gross, Francisco Massa, Adam Lerer, James Bradbury, Gregory Chanan, Trevor Killeen, Zeming Lin, Natalia Gimelshein, Luca Antiga, et al. Pytorch: An imperative style, high-performance deep learning library. *Advances in neural information processing systems*, 32, 2019.
- [40] Liangqiong Qu, Yuyin Zhou, Paul Pu Liang, Yingda Xia, Feifei Wang, Ehsan Adeli, Li Fei-Fei, and Daniel Rubin. Rethinking architecture design for tackling data heterogeneity in federated learning. In *Proceedings of the IEEE/CVF conference on computer vision and pattern recognition*, pages 10061–10071, 2022.
- [41] Sylvestre-Alvise Rebuffi, Alexander Kolesnikov, Georg Sperl, and Christoph H. Lampert. ICaRL: Incremental classifier and representation learning. In *2017 IEEE Conference on Computer Vision and Pattern Recognition (CVPR)*, pages 5533–5542, Honolulu, HI, July 2017. IEEE.
- [42] Youbang Sun, Zitao Li, Yaliang Li, and Bolin Ding. Improving lora in privacy-preserving federated learning. *arXiv preprint arXiv:2403.12313*, 2024.
- [43] Paul Voigt and Axel Von dem Bussche. The eu general data protection regulation (gdpr). *A Practical Guide, 1st Ed.*, Cham: Springer International Publishing, 10(3152676):10–5555, 2017.
- [44] Jianyu Wang, Zachary Charles, Zheng Xu, Gauri Joshi, H Brendan McMahan, Maruan Al-Shedivat, Galen Andrew, Salman Avestimehr, Katharine Daly, Deepesh Data, et al. A field guide to federated optimization. *arXiv preprint arXiv:2107.06917*, 2021.
- [45] Liyuan Wang, Xingxing Zhang, Hang Su, and Jun Zhu. A comprehensive survey of continual learning: theory, method and application. *IEEE Transactions on Pattern Analysis and Machine Intelligence*, 2024.
- [46] Zi Wang, Fei Wu, Feng Yu, Yurui Zhou, Jia Hu, and Geyong Min. Federated continual learning for edge-ai: A comprehensive survey. *arXiv preprint arXiv:2411.13740*, 2024.
- [47] Zifeng Wang, Zizhao Zhang, Chen-Yu Lee, Han Zhang, Ruoxi Sun, Xiaoqi Ren, Guolong Su, Vincent Perot, Jennifer Dy, and Tomas Pfister. Learning to Prompt for Continual Learning. In *2022 IEEE/CVF Conference on Computer Vision and Pattern Recognition (CVPR)*, pages 139–149, New Orleans, LA, USA, June 2022. IEEE.

- [48] Ziyao Wang, Zheyu Shen, Yexiao He, Guoheng Sun, Hongyi Wang, Lingjuan Lyu, and Ang Li. Flora: Federated fine-tuning large language models with heterogeneous low-rank adaptations. *arXiv preprint arXiv:2409.05976*, 2024.
- [49] Yichen Wu, Hongming Piao, Long-Kai Huang, Renzhen Wang, Wanhua Li, Hanspeter Pfister, Deyu Meng, Kede Ma, and Ying Wei. Sd-lora: Scalable decoupled low-rank adaptation for class incremental learning. In *The Thirteenth International Conference on Learning Representations*, 2025.
- [50] Xin Yang, Hao Yu, Xin Gao, Hao Wang, Junbo Zhang, and Tianrui Li. Federated continual learning via knowledge fusion: A survey. *IEEE Transactions on Knowledge and Data Engineering*, 36(8):3832–3850, 2024.
- [51] Gengwei Zhang, Liyuan Wang, Guoliang Kang, Ling Chen, and Yunchao Wei. Slca++: Unleash the power of sequential fine-tuning for continual learning with pre-training. *arXiv preprint arXiv:2408.08295*, 2024.
- [52] Jianyi Zhang, Saeed Vahidian, Martin Kuo, Chunyuan Li, Ruiyi Zhang, Tong Yu, Guoyin Wang, and Yiran Chen. Towards building the federatedgpt: Federated instruction tuning. In *ICASSP 2024-2024 IEEE International Conference on Acoustics, Speech and Signal Processing (ICASSP)*, pages 6915–6919. IEEE, 2024.
- [53] Jie Zhang, Chen Chen, Weiming Zhuang, and Lingjuan Lyu. TARGET: Federated Class-Continual Learning via Exemplar-Free Distillation. In *Proceedings of the IEEE/CVF International Conference on Computer Vision*, pages 4782–4793, 2023.
- [54] Zhuo Zhang, Yuanhang Yang, Yong Dai, Qifan Wang, Yue Yu, Lizhen Qu, and Zenglin Xu. FedPETuning: When Federated Learning Meets the Parameter-Efficient Tuning Methods of Pre-trained Language Models. In Anna Rogers, Jordan Boyd-Graber, and Naoaki Okazaki, editors, *Findings of the Association for Computational Linguistics: ACL 2023*, pages 9963–9977, Toronto, Canada, July 2023. Association for Computational Linguistics.
- [55] Yue Zhao, Meng Li, Liangzhen Lai, Naveen Suda, Damon Civin, and Vikas Chandra. Federated learning with non-iid data. *arXiv preprint arXiv:1806.00582*, 2018.
- [56] Da-Wei Zhou, Fu-Yun Wang, Han-Jia Ye, and De-Chuan Zhan. PyCIL: A Python Toolbox for Class-Incremental Learning. *Science China Information Sciences*, 66(9):197101, s11432–022–3600–y, September 2023.
- [57] Da-Wei Zhou, Qi-Wei Wang, Zhi-Hong Qi, Han-Jia Ye, De-Chuan Zhan, and Ziwei Liu. Class-incremental learning: A survey. *IEEE Transactions on Pattern Analysis and Machine Intelligence*, 2024.
- [58] Jiacheng Zhu, Kristjan Greenewald, Kimia Nadjahi, Hartz Sáez de Ocáriz Borde, Rickard Brühl Gabrielsson, Leshem Choshen, Marzyeh Ghassemi, Mikhail Yurochkin, and Justin Solomon. Asymmetry in low-rank adapters of foundation models. *arXiv preprint arXiv:2402.16842*, 2024.

## A Theory Analysis of LoRA-based Aggregation

Vanilla LoRA with direct weighted averaging introduces interference when deployed in federated learning scenarios with data heterogeneity [2, 42]. To understand this challenge, we first examine parameter aggregation in conventional federated learning. When fully-fine-tuning a PTM, the aggregated model parameters can be formulated as:

$$\mathbf{W} = \frac{1}{K} \sum_{k=1}^K \mathbf{W}_k, \quad (7)$$

where  $\mathbf{W}_k$  represents the trained weights from each client  $k$ . Ideally, with the assumption that the server could access all clients' datasets, the optimal global model  $\mathbf{W}_g^*$  when clients only tune LoRA locally can be expressed as:

$$\mathbf{W}_g^* = \frac{1}{K} \sum_{k=1}^K (\mathbf{W}_0 + \Delta \mathbf{W}_k) = \mathbf{W}_0 + \frac{1}{K} \sum_{k=1}^K (\mathbf{B}_k \mathbf{A}_k), \quad (8)$$

where  $\mathbf{W}_0$  is the frozen pre-trained weight in the PTM. However, the server aggregates the received LoRA matrices  $\mathbf{B}_k$  and  $\mathbf{A}_k$  independently in practical and challenging non-IID scenarios, resulting in

$$\hat{\mathbf{W}}_g = \frac{1}{K} \sum_{k=1}^K \mathbf{W}_k = \mathbf{W}_0 + \frac{1}{K} \sum_{k=1}^K \mathbf{B}_k \times \frac{1}{K} \sum_{k=1}^K \mathbf{A}_k. \quad (9)$$

This creates a critical discrepancy: in the presence of data heterogeneity, the average of matrix products is not equivalent to the product of average matrices, i.e.,  $\frac{1}{K} \sum_{k=1}^K (\mathbf{B}_k \mathbf{A}_k) \neq \frac{1}{K} \sum_{k=1}^K \mathbf{B}_k \times \frac{1}{K} \sum_{k=1}^K \mathbf{A}_k$ . Previous approaches to address this issue include: (1) updating the global model with the computed average of matrix products, which contradicts LoRA's purpose by requiring fine-tuning of expensive weight parameters; (2) keeping either matrix  $\mathbf{B}$  or matrix  $\mathbf{A}$  fixed [42, 58, 19], which reduces communication costs but limits model expressivity; or (3) using stacking-based aggregation [48], which achieves noise-free aggregation but incurs additional communication costs.

## B Implementation Details

In this section, we describe the implementation details of all experiments.

**Compute.** We run all experiments of all datasets on two GeForce RTX 3090 GPUs and two GeForce RTX 5090 GPUs.

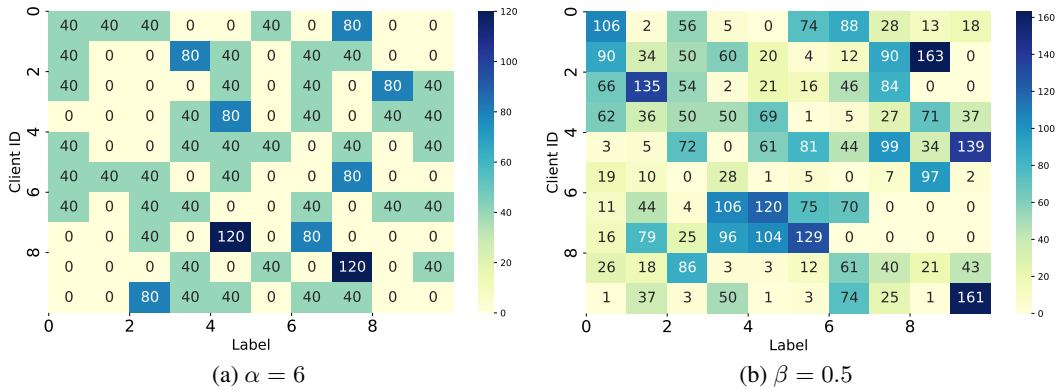


Figure 4: An example of the non-IID setting on CIFAR-100 dataset. The value in each rectangle is the number of data samples of a class belonging to a certain client.

**Datasets.** We use widely used datasets in the field of federated class-incremental learning, including (1) **CIFAR-100** [24]: This dataset comprises images from 100 classes. These classes are divided

into randomly 10 separate incremental tasks, with each task featuring a distinct set of classes. **(2) Tiny-ImageNet** [25]: This dataset is composed of images from 200 classes. It includes challenging examples from the original ImageNet [7]. These classes are also randomly divided into 10 distinct incremental tasks. **(3) ImageNet-Subset** [22]: This dataset contains the first 100 classes of the arranged 1,000 classes. For each task, we split the training data of the above three datasets into a training set and a validation set in an 8:2 ratio, and we evaluate the global model using a global test set. **(4) ImageNet** [7]: This dataset consists of 1,000 classes. For simplicity, we first preprocessed the dataset, i.e., keeping 700 images for each class. Then we split the training data of the dataset into a training set and a validation set in an 5:1 ratio, and evaluate the global model using a global test set.

**Various numbers of tasks.** Following [16], we obtain the main results from 10 tasks from all datasets. Additionally, to illustrate the scalability of our method with various different numbers of tasks, we also present the experimental results with 5 and 20 tasks for ImageNet-SubSet, Tiny-ImageNet.

**Non-IID settings.** As shown in Figure 4, we take CIFA-100 dataset as an example to illustrate the non-IID setting of our experiments. In the quantity-based label imbalance, we suppose each client only has data samples of  $\alpha$  different labels. We first randomly assign  $\alpha$  different label IDs to each client at each task. Then we randomly and equally divide them into the clients which own the label for the samples of each label. In the distribution-based label imbalance, we sample  $P_c$  from  $Dir_N(\beta)$  and allocate a  $P_{c,k}$  proportion of the samples of class  $c$  to the client  $k$ , where  $Dir(\cdot)$  denotes the Dirichlet distribution and  $\beta$  is a concentration parameter ( $\beta > 0$ ). The partition is more unbalanced if  $\beta$  is set to a smaller value.

**Baselines.** We compare our method against various baseline approaches including three categories:

1. Existing federated class-incremental learning methods.
  - GLFC [11]: elaborates a class-aware gradient compensation loss and a class-semantic relation distillation loss to address local oblivion caused by class imbalance at local clients and selects the best old global model with a proxy server to tackle global forgetting.
  - TARGET [53]: leverages the global model previously trained to transfer knowledge of old tasks to the current task while simulating the global distribution of data on each client with a generator.
  - LGA [10]: designs a local-global anti-forgetting model to synergistically solve the local and global catastrophic forgetting problem through a category-balanced gradient compensated loss and semantic distillation strategy.
  - PILoRA [16]: proposes prototype-guided incremental LoRA to mitigate catastrophic forgetting and data heterogeneity problems.
2. Several representative class-incremental learning methods adapted to FL settings.
  - EWC [23]: fine-tune the whole model with a regularization loss that prevents updating parameters that could interfere with previously learned tasks.
  - LwF [31]: constrains the shared representation layer to be similar to its original state before learning the new task.
  - iCaRL [41]: combines mean prototype classification, prioritized sample selection, and distillation-assisted representation learning to solve the catastrophic forgetting of deep neural networks.
  - L2P [47]: uses the input to dynamically select and update prompts from the prompt pool in an instance-wise fashion.
3. Several common federated learning methods adapted to CIL settings.
  - FedNCM [28]. proposes a two-stage process consisting of HeadTuning followed by fine-tuning to achieve faster convergence and higher accuracy without violating FL constraints.

**Metrics.** Let  $FAA$  denotes the average accuracy of all classes after learning the final task. Let  $S_{t,\tau}$  denotes the classification accuracy on the  $\tau$ -th task after training on the  $t$ -th task.

$$FAA = A_T, A_t = \frac{1}{t} \sum_{\tau=1}^t S_{t,\tau}, \quad (10)$$

where  $A_t$  denotes the average accuracy up to the  $t$ -th task and  $T$  is the total number of all tasks. Accordingly, the formal definition of  $AIA$  can be formulated as:

$$AIA = \frac{1}{T} \sum_{t=1}^T A_t. \quad (11)$$

## C Impact of Task-agnostic LoRA Placements

In this appendix, we investigate the impact of task-agnostic LoRA placements across different transformer blocks, including whether to incorporate LoRA in FFN (also called MLP) layers.

### C.1 Exploration regards to task-agnostic LoRA embedded in specific blocks

To evaluate how task-agnostic LoRA placement affects model performance, we conducted experiments with different configurations. For CIFAR-100, we compared three placement strategies: the first 4 blocks (denoted as **first**), middle 4 blocks (**mid**), and last 4 blocks (**last**). Results are presented in Figure 5. Similarly, for Tiny-ImageNet, we compared two strategies: the first 6 blocks (**bottom**) and the last 6 blocks (**top**), with results shown in Figure 6. Our findings consistently demonstrate that models with task-agnostic LoRA placed in the lower transformer blocks (**first** for CIFAR-100 and **bottom** for Tiny-ImageNet) achieve superior performance compared to other configurations. Considering the resource usage analysis presented in Section 5.2.3, we conclude that these lower block placement strategies represent the optimal design choice for their respective datasets, balancing model quality, computational cost, and memory consumption during inference.

Table 6: Analysis of different task-agnostic LoRA placements on CIFAR-100.

Method	$\alpha = 6$		$\beta = 0.5$	
	$FAA$	$AIA$	$FAA$	$AIA$
Ours (block 1, w/ MLP)	69.1	78.3	71.0	81.2
Ours (block 1, w/o MLP)	70.7	79.5	72.1	82.0
Ours (block 1-4, w/ MLP)	76.6	84.2	77.4	85.5
Ours (block 1-4, w/o MLP)	76.4	83.9	77.3	85.4
Ours (block 1-12, w/ MLP)	76.7	84.2	77.6	85.7

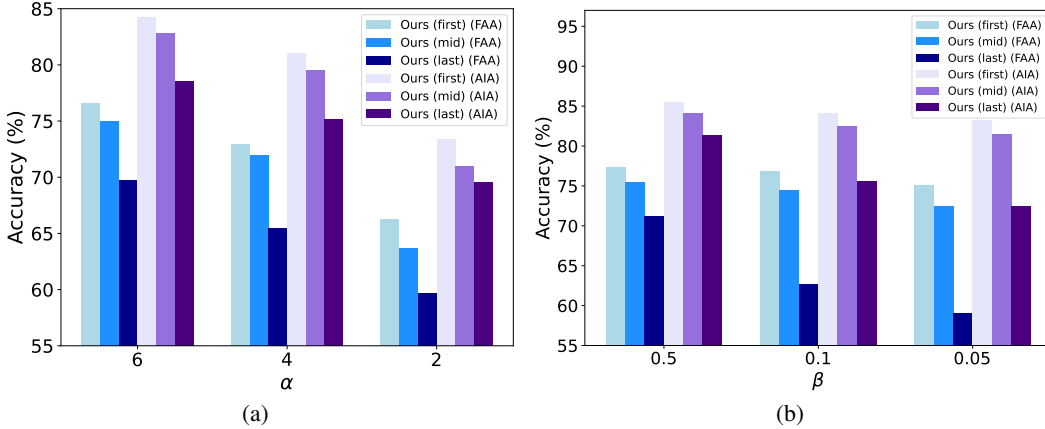


Figure 5: Model performance of LoRA embedded in different blocks for CIFAR-100 dataset.

### C.2 Exploration of LoRA placement in MLP layers

To investigate the optimal placement of task-agnostic LoRA parameters in attention and MLP layers, we conducted comprehensive experiments across CIFAR-100 and Tiny-ImageNet datasets. Table 6 and 7 present our results, demonstrating that our approach of fine-tuning LoRA parameters in the first



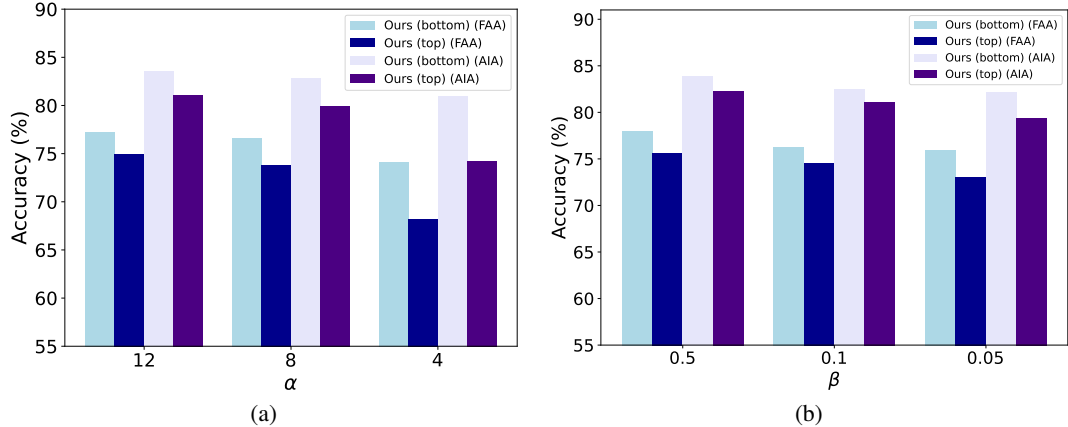


Figure 6: Model performance of LoRA embedded in different blocks for Tiny-ImageNet dataset.

Table 7: Analysis of different task-agnostic LoRA placements on Tiny-ImageNet.

Method	$\alpha = 12$		$\beta = 0.5$	
	FAA	AIA	FAA	AIA
Ours (block 1, w/ MLP)	72.9	80.6	74.4	81.7
Ours (block 1, w/o MLP)	73.3	80.3	74.5	81.8
Ours (block 1-4, w/ MLP)	77.1	83.0	77.8	84.0
Ours (block 1-4, w/o MLP)	77.2	82.8	77.3	83.6
Ours (block 1-6, w/ MLP)	77.2	83.0	78.0	83.9
Ours (block 1-12, w/ MLP)	78.0	84.0	78.2	84.2

transformer block (denoted as *Ours (block 1, w/ MLP)*) marginally outperforms the current SOTA PiLoRA method, with detailed performance metrics available in Table 1.

Our experiments reveal intriguing patterns regarding MLP layer inclusion. When restricting LoRA to only the first block, excluding MLP layers yields superior performance on both datasets. However, when extending LoRA across block 1-4, including MLP layers consistently delivers better results. We attribute these observations to two key factors: **(1)** When fine-tuning a limited parameter set (as in *Ours (block 1, w/ MLP)* and *Ours (block 1, w/o MLP)*), attention layer weights contribute more significantly to model performance than MLP layer weights; **(2)** With an expanded parameter space (comparing *Ours (block 1-4, w/ MLP)* and *Ours (block 1-4, w/o MLP)* to their block 1 counterparts), the inclusion of MLP layers provides complementary benefits that enhance multi-layer LoRA fine-tuning effectiveness.

Further evidence from Figures 5 and 6 suggests a hierarchical feature extraction mechanism, where lower blocks capture coarser features while upper blocks extract finer details. Notably, our experiments confirm that fine-tuning LoRA across all transformer blocks consistently achieves optimal performance, reinforcing previous findings by [14, 33] that involving more critical parameters in Vision Transformers during training yields superior results, albeit at increased computational and communication costs.

## D Extended Results

In this appendix, we report more extended results on ImageNet-Subset [22], Tiny-ImageNet [25] and ImageNet [7].

### D.1 Results on ImageNet-Subset and Tiny-ImageNet

To validate the superior performance of Fed-TaLoRA for 5/10/20 tasks (20/10/5 classes per task), we conducted qualitative analysis on ImageNet-Subset dataset, as shown in Table 8 and Figure 8.

According to these curves, we can easily observe that Fed-TaLoRA performs much better than the current SOTA method PILoRA in the two different non-IID settings when  $T = 5, 10$  but obtain slightly worse than PILoRA when  $T = 20$ . We attribute this to coarse Fed-TaLoRA can not capture abundant class representations for each task containing fewer classes, but PILoRA can work better since it extract class-specific prototypes for each class in per task, which is a finer-grained representation process at a much higher resource costs including computation, memory and communication.

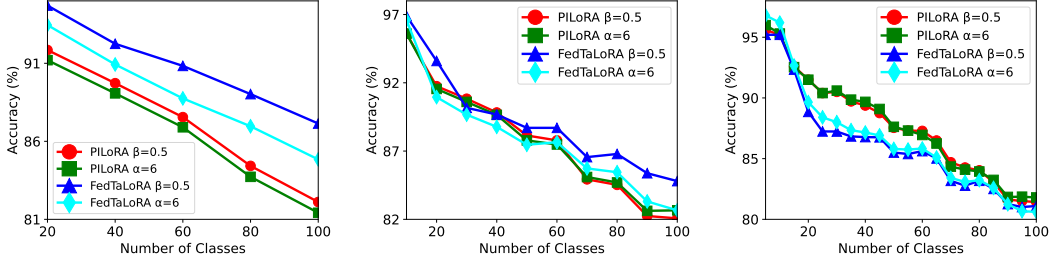


Figure 7: Qualitative analysis of different incremental tasks on ImageNet-Subset [22] when  $T = 5$  (top),  $T = 10$  (middle) and  $T = 20$  (bottom).

Table 8: Qualitative analysis on ImageNet-Subset including 5/10/20 tasks (20/10/5 classes per task).

Method	$T = 5$				$T = 10$				$T = 20$			
	$\alpha = 6$		$\beta = 0.5$		$\alpha = 6$		$\beta = 0.5$		$\alpha = 6$		$\beta = 0.5$	
	FAA	AIA	FAA	AIA	FAA	AIA	FAA	AIA	FAA	AIA	FAA	AIA
PILoRA	81.4	86.5	82.1	87.1	82.7	87.8	82.1	87.8	81.8	87.7	81.9	87.8
<b>Fed-TaLoRA</b>	84.8	89.0	87.1	90.8	82.7	87.9	84.8	89.1	80.6	86.5	81.1	86.2

Furthermore, we conduct extended experiments on Tiny-ImageNet with 5/10/20 tasks (40/20/10 classes per task). As shown in Table 9 and Figure 7, Fed-TaLoRA performs much better than PILoRA in all heterogeneous data scenarios. Therefore, these demonstrate Fed-TaLoRA can largely enhance the model performance combining TaLoTA and ResWU mechanism, further emphasizing the potential of *task-agnostic adaptation* and *post-aggregation model calibration*.

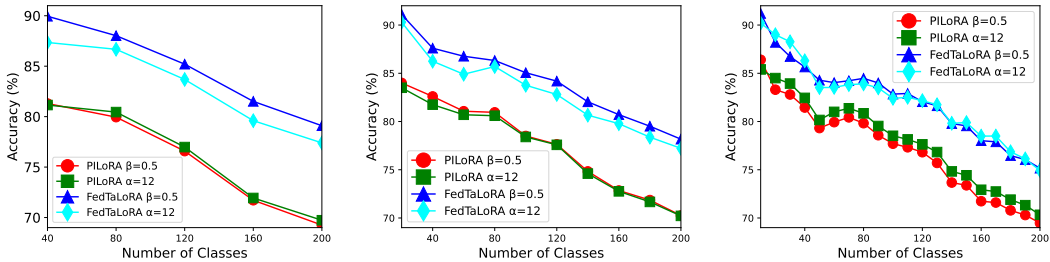


Figure 8: Qualitative analysis of different incremental tasks on Tiny-ImageNet [25] when  $T = 5$  (top),  $T = 10$  (middle) and  $T = 20$  (bottom).

## D.2 Results on ImageNet

To evaluate our model’s scalability to larger datasets, we conducted comprehensive experiments on ImageNet. As shown in Table 10, even our minimal variant—with task-agnostic LoRA embedded only in the first transformer block—significantly outperforms PILoRA. These results demonstrate not only the effectiveness of our approach to complex, large-scale datasets but also highlight promising opportunities for further optimization of the efficiency-performance trade-off. The strong performance with such limited parameter adaptation suggests that strategic LoRA deployment can achieve superior results while maintaining minimal resource requirements, reinforcing Fed-TaLoRA’s scalability

Table 9: Results (%) on Tiny-ImageNet including 5/10/20 tasks (40/20/10 classes per task).

Method	$T = 5$				$T = 10$				$T = 20$			
	$\alpha = 12$		$\beta = 0.5$		$\alpha = 12$		$\beta = 0.5$		$\alpha = 12$		$\beta = 0.5$	
	<i>FAA</i>	<i>AIA</i>	<i>FAA</i>	<i>AIA</i>	<i>FAA</i>	<i>AIA</i>	<i>FAA</i>	<i>AIA</i>	<i>FAA</i>	<i>AIA</i>	<i>FAA</i>	<i>AIA</i>
PILoRA	69.7	76.1	69.3	75.8	74.4	81.0	74.5	80.9	70.3	77.9	69.5	77.0
<b>Fed-TaLoRA</b>	77.4	82.9	79.1	84.8	77.2	83.0	78.0	83.9	74.9	82.3	75.2	82.3

potential for real-world applications with varying computational constraints, since it eliminates the additional costs as the number of tasks grows [49].

Table 10: Results (%) on ImageNet including 10 tasks (100 classes per task).

Method	$\alpha = 60$		$\beta = 0.5$	
	<i>FAA</i>	<i>AIA</i>	<i>FAA</i>	<i>AIA</i>
PILoRA	68.0	73.6	67.3	72.8
Ours (block 1, w/ MLP)	73.3	78.9	74.5	80.6
Ours (block 1, w/o MLP)	72.9	78.5	74.6	80.6
Ours (block 1-6, w/ MLP)	73.5	79.0	74.8	80.7

## E Training Curves

We plot some selected training curves for  $T = 5$  (Figure 9),  $T = 10$  (Figure 10) and  $T = 20$  (Figure 11) on Tiny-ImageNet when  $\alpha = 12$ , and  $T = 10$  (12) on Tiny-ImageNet when  $\beta = 0.5$ . We can see that our model can converge at different tasks' lengths representing the complexity of downstream tasks regardless of distribution-based label imbalance or quantity-based label imbalance.

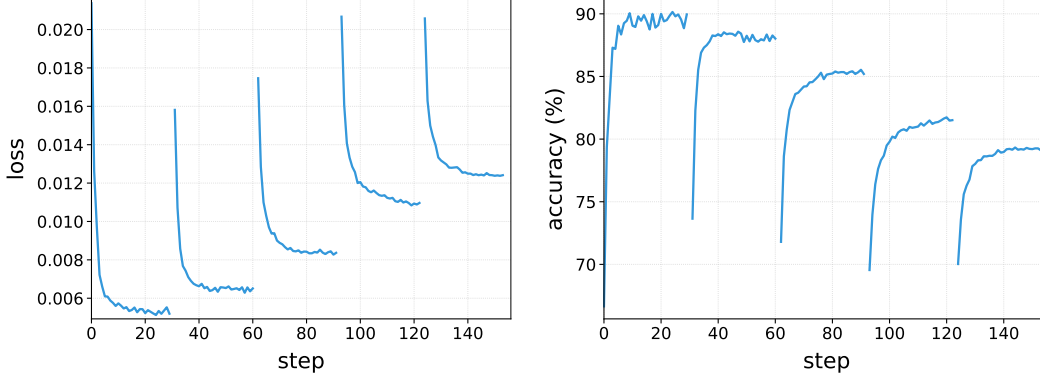


Figure 9: Training curves for  $T = 5$  on Tiny-ImageNet when  $\alpha = 12$ .

## F Limitations

Firstly, we utilize the self-supervised pre-trained weights of DINO [4] for ViT-B/16 [12] as the backbone for the image classification tasks in the FCIL setup. More future work can be made with Fed-ToLoRA to explore more Transformer-derived models and sizes over various datasets. Secondly, although we explored the impact of the ResWU mechanism on the global convergence of the model, it is an interesting and important future direction, which can further reveal the nature of how our approach works in different heterogeneous data scenarios.

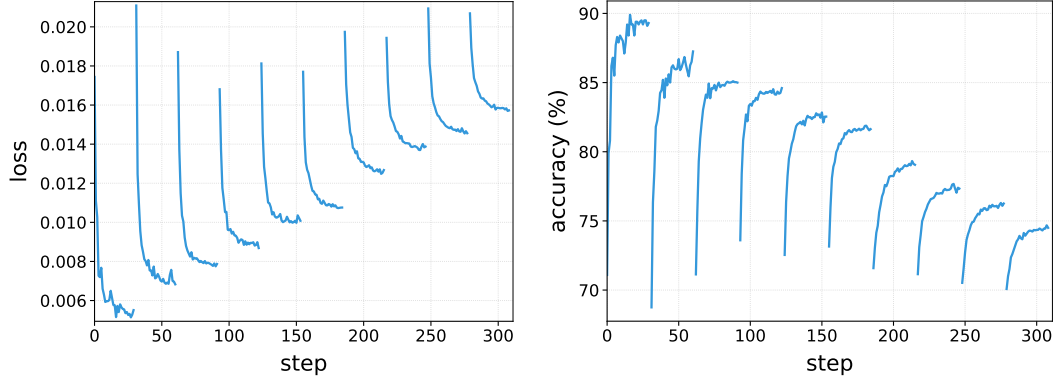


Figure 10: Training curves for  $T = 10$  on Tiny-ImageNet when  $\alpha = 12$ .

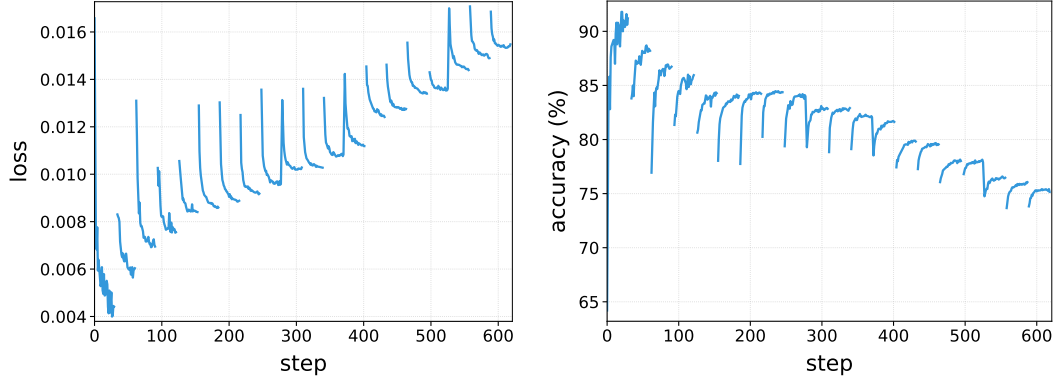


Figure 11: Training curves for  $T = 20$  on Tiny-ImageNet when  $\alpha = 12$ .

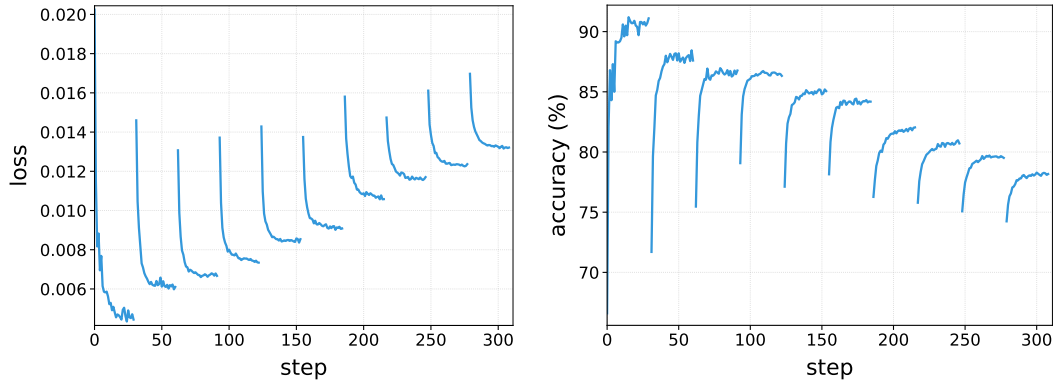


Figure 12: Training curves for  $T = 10$  on Tiny-ImageNet when  $\beta = 0.5$ .